Research Article

Nano Biomed Eng

RNAi Degrades the SARS-CoV-2 Spike Protein RNA for Developing Drugs to Treat COVID-19

Weiwei Zhang[1,2,3], Linjia Huang[2], Jumei Huang[2], Xin Jiang[3,4], Xiaohong Ren[6], Xiaojie Shi[1], Ling Ye[2,3], Shuhui Bian[4], Jianhe Sun[2], Yufeng Gao[2], Zehua Hu[2], Lintin Guo[2], Suyan Chen[4], Jiahao Xu[2], Jie Wu[1,3], Jiwen Zhang[3,6]✉, Daxiang Cui[5]✉, Fangping Dai[1,2,3,5]✉

[1]Central Laboratory, Nantong Haimen People's Hospital, Nantong 226199, China.
[2]Genome-decoding Biomedical Technology Co., Ltd., Nantong 226126, China.
[3]Yangtze Delta Drug Advanced Research Institute, Nantong 226126, China.
[4]Precision-genes Bio-Technology Co., Ltd/Medical Laboratory, Nantong 226126, China.
[5]National Engineering Research Center for Nanotechnology, Shanghai Jiao Tong University, Shanghai 200241, China.
[6]Shanghai Institute of Materia Medica, Chinese Academy of Sciences, Shanghai 201203, China

✉ Corresponding authors. E-mail: dfp@genomedecoding.com;dxcui@sjtu.edu.cn;jwzhang@simm.ac.cn
Tel: +86 13761307585 Fax: 0086-513-68067951

Received: Oct. 21, 2022; **Accepted:** Nov. 7, 2022; **Published:** Nov. 7, 2022

Citation: Weiwei Zhang, Linjia Huang, Jumei Huang, Xin Jiang, Xiaohong Ren, Xiaojie Shi, Ling Ye, Shuhui Bian, Jianhe Sun, Yufeng Gao, Zehua Hu, Lintin Guo, Suyan Chen, Jiahao Xu, Jie Wu, Jiwen Zhang, Daxiang Cui, and Fangping Dai, RNAi Degrades the SARS-CoV-2 Spike Protein RNA for Developing Drugs to Treat COVID-19. *Nano Biomed. Eng.*, 2022, 14(2): 173-185.
DOI: 10.5101/nbe.v14i2.p173-185.

Abstract

COVID-19 is caused by severe acute respiratory SARS-CoV-2. Regardless of the availability of treatment strategies for COVID-19, effective therapy will remain essential. A promising approach to tackle the SARS-CoV-2 could be small interfering (si) RNAs. Here we designed the small hairpin RNA (named as shRNA688) for targeting the prepared 813 bp Est of the S protein genes (Delta). The conserved and mutated regions of the S protein genes from the genomes of the SARS-CoV-2 variants in the public database were analyzed. A 813 bp fragment encoding the most part of the RBD and partial downstream RBD of the S protein was cloned into the upstream red florescent protein gene (RFP) as a fusing gene in the pCMV-S-Protein RBD-Est-RFP plasmid for expressing a potential target for RNAi. The double stranded of the DNA encoding for shRNA688 was constructed in the downstream human H1 promoter of the plasmid in which CMV promoter drives enhanced green fluorescent protein (EGFP) marker gene expression. These two kinds of the constructed plasmids were co-transfected into HEK293T via Lipofectamine 2000. The degradation of the transcripts of the SARS-CoV-2 S protein fusing gene expressed in the transfected HEK293T treated by RNAi was analyzed by RT-qPCR with a specific probe of the targeted SARS-CoV-2 S protein gene transcripts. Our results showed that shRNA688 targeting the conserved region of the S protein genes could effectively reduce the transcripts of the S protein genes. This study provides a cell model and technical support for the research and development of the broad-spectrum small nucleic acid RNAi drugs against SARS-CoV-2 or the RNAi drugs for the other hazard viruses which cause human diseases.

Keywords: COVID-19, RNAi, Nanoparticles, shRNA, Plasmids

Introduction

The global coronavirus disease 19 (COVID-19) pandemic is caused by severe acute respiratory syndrome coronavirus 2 (SARS-CoV-2) [1]. The virus has a higher rates human-to-human transmission rate, facilitating rapid spread across the world [2]. According to the John Hopkins coronavirus resource center, SARS-CoV-2 has infected over 200 million people and caused more than 4.5 million deaths

worldwide till September 2021 [3]. Vaccines are markedly slowing the increase in positive cases and deaths; however, vaccination may not cover the global population fully [4]. Furthermore, mutated variant strains of SARS-CoV-2 that escaped from immunity in response to previous infection or vaccination are continuously emerging, and causing new local and global outbreaks [5, 6]. The emergence of Omicron variant indicates how fast the SARS-CoV-2 evolves, and its potential impact on the current protein-based intervention (i.e., vaccines, antibodies, or convalescent plasma) that primarily targets the highly mutated Spike (S) protein cannot be neglected [7]. One emerging concept in anti-COVID-19 medication involves the development of nucleic acid-based therapeutics, which can degrade the viral genome and can be quickly adjusted to viral mutations [8-10]. Nucleic acid-based therapeutics include small interfering RNAs (siRNAs). These are about 19~21 base-pair long, noncoding RNA duplexes that can knockdown the expression of target genes in a sequence-specific way by mediating targeted mRNA degradation [11, 12]. After cellular uptake, the siRNA duplex is loaded into the RNA-induced silencing complex (RISC). The duplex is processed to a single strand that binds with high specificity to complementary RNAs present in the cytosol, resulting in their cleavage [12, 13]. The ongoing pandemic prompted multiple research groups to evaluate siRNA-based therapies for COVID-19. While the most of the published studies so far reviewed the potential of RNAi to treat COVID-19 [14-17], describe in-silico studies [18, 19], initial proof-of-concept that SARS-CoV-2 can be inhibited by siRNAs was also provided [8, 20, 21]. The designed siRNA targeting the Orf1a/b region of the SARS-CoV-2 RNA genome, encoding for non-structural proteins (nsp), was tested. A siRNA with highly efficient inhibition of SARS-CoV-2 replication was identified [19, 22]. The adeno-associated virus vectors co-expressing a cocktail of the short hairpin RNAs (shRNA) directed against the SARS-CoV-2 RdRp and N genes were tested. The results indicated RNAi has the potential and promising drug candidate for therapeutic intervention [23]. An in-depth understanding of an efficient suppression of viral replication would be a requirement to formulate a potent antiviral strategy [24].

The SARS-CoV-2 is an enveloped, single-stranded large RNA virus, with a 5' untranslated region (UTR), the ORF1a/b RNA encoding non-structural viral proteins, and a 3' segment encoding the structural proteins, such as the S protein that binds to the human angiotensin-converting enzyme 2 (hACE2) receptor on host cells, and the nucleocapsid N protein involved in virion assembly [25], and a 3' UTR [2, 26]. As a global response to the COVID-19 pandemic, the large amount of genomes of the SARS-CoV-2 variants, including the sequences of the S protein genes and proteins of the SARS-CoV-2 variants are available in the public database (https://www.ncbi.nlm.nih.gov/nuccore/?Term=SARS-CoV-2%2C+S+ protein) [27, 28]. The dynamic properties of the S protein, particularly the much more transmissible Delta and Omicron variants were reported. The more mutations have accumulated in the Omicron S proteins, including the RBD [29,30]. The mutations in the receptor-binding domains (RBDs) of the S protein influence its affinities to ACE2 [31]. The SARS-CoV-2 have the large RNA genome but without integration in human genome as they replicate in the cell cytoplasm of the human lung epithelial cells [32]. The antiviral efficacy of adenosine-based analogs, the main repurposed drugs for SARS-CoV-2 RNA-dependent RNA polymerase inhibition was investigated [33]. Using nucleic acid antisense oligonucleotides were described as a potential novel therapeutic strategy targeting the SARS-CoV-2 RNA. An antisense oligonucleotide binding to the 5′ leader sequence of the SARS-CoV-2 disrupted a highly conserved stem-loop structure with nanomolar efficacy in preventing viral replication in human cells [2].

Here we designed the small hairpin RNA (named as shRNA688) for targeting the prepared 813 bp Est of the S protein genes (Delta) after cluster analysis. The conserved and mutated regions of the S protein genes of the genomes of the SARS-CoV-2 variants from the public database were analyzed. A 813 bp fragment encoding for the most part of the RBD and partial downstream RBD of the S protein (Delta) was cloned into the upstream red florescent protein gene (RFP) as a fusing gene expressing as a potential target for RNAi testing as the pCMV-S-Protein RBD-Est-RFP plasmid. The double stranded of the DNA shRNA688 were constructed in the downstream human H1 promoter of a plasmid which could also express green fluorescent protein (EGFP) marker gene. The dual expression of the EGFP and shRNA in a plasmid was convenient way to understand to transfection efficiency (34). These two kinds of the constructed plasmids were co-transfected into HEK293T *via* Lipofectamine 2000. The degradation of SARS CoV-2 S protein gene fragment transcripts expressed in the transfected HEK293T after

RNAi treatment was studied by analyzing the image of gene transfected cells and the fluorescence quantitative reverse transcription polymerase chain reaction (RT qPCR) data using a specific probe targeting SARS CoV-2 S protein gene.

Experimental

Selection of RNAi targets by analysis the conserved and mutant sequences of SARS-CoV-2 variants

The multiple genome and S protein sequences from SARS-CoV-2 variants, alpha, beta, gamma, delta, and omicrons were obtained from the Genbank (https://www.ncbi.nlm.nih.gov/nuccore/?term=SARS-CoV-2). The clustal comparisons were performed by the online tool of the UCSC genome browser for SRAS-CoV-2 (http://genome.ucsc. edu/cgi-bin/hgBlat), the Clustal Omega (https://www.ebi.ac.uk/Tools/msa/clustalo/). The conserved region was selected on the consensus of the S protein genes of the SRAS-CoV-2. The sense sequence (21 bp) was picked up for the shRNA, which was as same as the targeted sequence of the S protein genes of the SRAS-CoV-2. After the sense sequence (21 bp), there was a loop sequence with "TTCAAGAGC". After that, there were a fragment of reverse complementary (21 bp) and a fragment of poly$(T)_6$. Then, a shRNA contained the elements, a sense, a loop, an antisense, and a poly$(T)_6$. The designed shRNA688 sequence and the complementary sequence were in the list (Table 1).

Construction of H1-shRNA688-pCMV-EGFP plasmid

For construction of the shRNA expression plasmid, a pSIL-EGFP vector https://www.addgene.org/52675/sequences/) contained pCMV-EGFP gene for gene transfection marker gene was used as the basic vector. The human RNA polymerase III type promoters (34), H1 promoter (108 bp) was constructed in the upstream of the pCMV-EGFP regions *via* XhoI and HindIII construction sites. The shRNA688 was integrated in downstream the promoters, H1 promoter (108 bp) *via* HindIII and EcoRI restriction sites. The constructed plasmid was confirmed by Sanger sequencing.

Selection and Preparation of the RBD containing Fragment of the SARS CoV-2 Delta S Protein Gene

Based on cluster analysis of the S protein sequences from the SARS-CoV-2 variants, a fragment (813 bp) of an RBD containing sequence (EST) from the S protein of the SARS-CoV-2 Delta variant was selected. This is a region that not only contains the special mutation in SARS CoV-2 Delta S protein gene, but also contains the shared conservative region in Omicron B.1, B.5 and other SARS CoV-2 S protein genes. For construction of this S protein RBD containing EST expression plasmid, this fragment sequence (813 bp) as a sense strand and its reverse complementary as an antisense strand with added few nucleoside acids at both ends were synthesized. After the sense and the antisense strands were annealed as a double strands of DNA fragment with the sticky restriction sites, for XhoI at 5'end and KpnI at 3'end, were formed.

Construction of an RBD containing fragment of the SARS-CoV-2 S protein and RFP fusing gene expression plasmid

The pLVX-IRES-mCherry vector (Takara Bio USA), which contains the CMV promoter, multiple cloning sites (MCS), mCherry red fluorescent protein (RFP) gene with polyA tail, was used as the basic vector for expression of the RBD containing EST of the S protein gene of the SARS-CoV-2. In this vector MCS, there are the restriction sites of XhoI (2809) and SacII (2834). There are two SacII and two KpnI restriction sites in the vector. Their cutter positions are in a way as SacII (2834) - KpnI (3289) -SacII (4644) – KpnI (4869). For construction, this empty vector was double digested with enzymes, XhoI and SacII (Takara Bio USA). The circle vector was first opened with XhoI. The digested vector DNA was harvested from 0.8% agarose gel. The recovered DNA was further digested by Sac II. The two fragments from the double digested vector were separated on 1% agarose gel (Shanghai Yuanye Bio-Technology Co., Ltd). The big fragment (6322 bp) was with SacII sticky end (5')

Table 1 The oligo sequences for constructing the shRNA688 expression plasmid

Oligo names	Sequences
nRBD-4F-688	AGCTTGGTGTTCTTACTGAGTCTAACTTCAAGAGCGTTAGACTCAGTAAGAACACCTTTTTTG
nRBD-4R-688	AATTCAAAAAAGGTGTTCTTACTGAGTCTAACGCTCTTGAAGTTAGACTCAGTAAGAACACCA

and XhoI sticky end (3'). The second fragment (1816 bp) was with SacII sticky end at both ends. The second fragment (1816 bp) was further digested with KpnI to result in two sub-fragments (1316 bp, 459 bp). The two sub-fragments were further separated on 1.5% agarose gel. The fragment (1316 bp) with KpnI sticky end (5') and SacII sticky end (3') was harvested from the gel. Then, three fragments, two of them (6322 bp and 1316 bp) from the pLVX-IRES-mCherry vector, and one of them, the double strands of the DNA fragment, which was encoding the most of the RBD and partial downstream RBD of S protein of SARS-CoV-2, were with XhoI and KpnI sticky-ends (825 bp), connected and circled by T4 DNA ligase (5 u/μL) (Thermo Fisher Scientific) as an expression plasmid. The constructed plasmid is called pCMV-S protein RBD-EST-RFP. The insertion region of plasmid was confirmed by Sanger sequencing (Fig. 1).

Transfection of the S protein RBD containing fragment and RFP fusing gene expression plasmid, shRNA and EGFP plasmid to HEK293 cells

The human cell line, HEK293T cells (ATCC) were cultured in high-glucose Dulbecco's Modified Eagle Medium (Thermo Fisher Scientific) supplemented with 10% fetal bovine serum (FBS), 1% antibiotics (100 μg/mL penicillin, 100 μg/mL streptomycin), 2 mM glutamine, and 1.5 mg/mL sodium bicarbonate at 37 °C in a humidified incubator with 5% CO_2 (All reagents were obtained from Thermo Fisher Scientific). The sub-cultured HEK293T cells were used for transient transfection experiments. The cell suspension was diluted to 1×10^5 cells/mL and seeded in 6-well-plates When the cells were grown reaching 70% confluence, then washed with phosphate buffered saline (PBS). Either constructed pCMV-S-protein RBD-EST-RFP or the pH1-shRNA-EGFP plasmids was transiently transfected into the cultured HEK293T cells mediated with the transfection reagent, Lipofectamine 2000, according to the manufacturer protocol. Briefly, each transfection mix was prepared in serum-free DMEM with 1 μg/100 μL of a DNA plasmid and 3 μL Lipofectamine 2000 as ratio of 1:3. One mix for each transfection was agitated in 200 μL and incubated 15 min at room temperature. An equal mass of shRNA or control plasmid was used for these respective transfections. The mixes were added to the cells in 0.5 mL per a well in 6-well plates and incubated for 6-20 h. After that, the mixes were removed from the treated cells, and the 1.5 mL/well normal growth DMEM supplemented with 10% FBS, 1% antibiotics were subsequently added back to the treated cells.

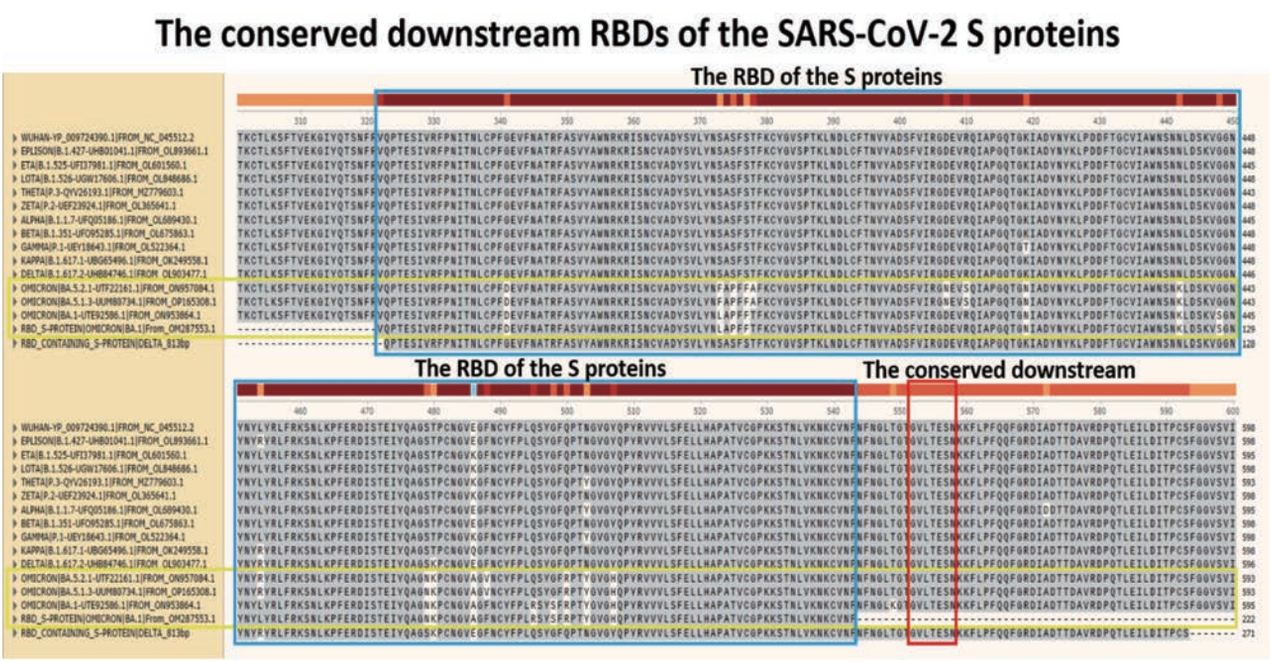

Fig. 1 Cluster analyzing of the RBD regions of the S proteins of SARS-CoV-2 variants. Each RBD region has at least one mutation in peptide level shown in the blue boxes of the two blocks. In the blocks, the mutations (with white background) of the peptide sequences are shown from different S protein RBD isoforms of SARS-CoV-2 variants, including the Omicron variants within the yellow boxes. In the last line, the sequence of the RBD containing and partial downstream RBD was from Delta, and its 813 nt cDNA was selected for integrating to an RFP gene over-expression plasmid as the shRNA targets in this study. The peptides in red box in downstream RBDs are highly conserved in all variants without any mutation.

Table 2 The primers and probes for RT-qPCR to detect SARS-CoV-2 S protein RBD EST degraded by the shRNA

Oligo names	Sequences (within S protein RBD region)
qPCR-13R-nRBD-688-174bp primer 5'	AGCAACTGTTTGTGGACCTAA
qPCR-13F-nRBD-688-174bp primer 3'	TGGTGTAATGTCAAGAATCTCAAGTG
RBD-Taqman probe-4	TGTGGATCACGGACAGCATCAGT (reverse)

Fluorescence image analysis of transfected cells expressing the S protein RBD-RFP fusion gene, shRNA and EGFP gene

The transgenic expressions were examined and validated 24 hours after the transfection under fluorescence microscope. The red or green, fluorescent cells were visualized by fluorescence microscopy on a microscope (10X magnification, DMIL LED, Leica, Germany). The fluorescent cells (the red or/and green fluorescence) over the total cells (under normal light) were observed. The images were taken. The overlapping or co-localized RFP and EGFP images were performed to understand the double transfection efficiency using the software matched to the microscope images.

Nucleic acid extraction and strand-specific cDNA synthesis

For quantitative RT-PCR, the total RNA was extracted from the transfected cells 24 hours post transfection with the FastPure Cell/Tissue Total RNA isolation Kit V2 (Vazyme RC112, China). The cells in each well were lysed with the buffer from the Kit. After then, the subsequent steps were performed according to the manufacturer's instructions. The quality and concentration of the eluted total RNA from each sample was measured by Nanodrop 2000 spectrophotometer (Thermo Scientific, Waltham, MA, USA); Samples with A260/280 ratios between 1.8 and 2.2 were considered for next steps. cDNAs were prepared from 1 μg total RNA using the HiScript III 1st Strand cDNA Synthesis Kit (+gDNA wiper) (Vazyme R312-01/02, China) and oligo (dT) as primer for 60 min at 45 °C.

Quantitation of the targeted SARS-CoV-2 transcripts *via* RT-qPCR

The quantitation of SARS-CoV-2 S protein RBD-EST and housekeeping gene transcripts in the transfected cell cultures were carried out with a RT-qPCR. Total RNA and cDNAs were prepared as described above. A RT-qPCR was conducted using the AceQ Universal U+ probe Master Mix V2 (Vazyme Q513, China). For each reaction, 10 μL "2X AceQ Universal U+ Probe Master Mix V2", 0.4 μL the sense primer (10 μM), 0.4 μL the antisense primer (10 μM), the targeting S protein RBD specific probe (10 μM), and the sample cDNA with ddH2O, a total volume was 20 μL. The primers and targeting S protein RBD specific probes were designed, used and listed in the Table 2. The cycle conditions of the RT-qPCR were applied as an incubation step at 37 °C for 2 min, an initial denaturation step at 95 °C for 5 min, followed by 45 cycles of amplification for 10 s at 95 °C and 30 s at 60 °C using a Light Cycler 480 (Roche, Basel, Switzerland). The quantities of the transcripts were normalized by the amount of GAPDH transcript. Relative quantification of the targeted RBD EST degraded by the tested shRNA688 was calculated using the standard $2^{-\Delta Ct}$ method.

Results and Discussion

The mutant and conserved regions of S protein RBD of the SARS-CoV-2 variants

One published SARS-CoV-2 Spike protein (S protein, surface glycoprotein isoform, YP_009724390) is composed of the 1273 amino acids. Among them, the 223 amino acids (319-541) are for the receptor-binding domain (RBD). The RBD is for the binding to human ACE2 (https://www.uniprot.org/uniprotkb/P0DTC2). Taking the cDNA and protein sequences of this S protein and its RBD as the references, the sequences of the S protein genes and their translated protein isoforms of the SARS-CoV-2 variants were cluster analyzed. The results showed that there was at least one amino acid mutation in each of the RBDs of the S protein isoforms. There were several mutations in Omicrons BA.1, BA5.1.3, BA.5.2.1. However, the conserved regions were remained which have no mutation in downstream RBDs. In this study, an 813nt cDNA sequence encoding for the most part of the RBD region and the partial downstream RBD of the SARS-CoV-2 Delta S protein was selected (Fig.1). This cDNA sequence and its reverse complementary

sequence were synthesized and annealed as a fragment which was integrated with the RFP cDNA as a fusing gene in the pCMV-RFP expression plasmid.

The constructed S protein RBD EST of SARS-CoV-2 Delta and RFP fusing gene

The RBD EST of the S protein of the SARS-CoV-2 Delta and mCherry red fluorescent protein (RFP) fusing gene was constructed in pLVX-IRES-mCherry RFP plasmid for expressing the potential target to evaluate the effectiveness of the shRNA interference. In this pLVX-IRES-mCherry plasmid, pCMV drives mCherry RFP gene expression. We removed the most part of the IRES between the restriction sites of XhoI and KpnI. The synthesis and annealed double strands of the DNA fragment was with the sense strand (813 nt) encodes for the most part of the S protein RBD of the SARS-CoV-2 Delta S protein was successfully integrated into this plasmid (Figure 2). The 813 nt insert integrating with RFP gene as a fusing gene was approved by Sanger sequencing. The insert theoretically encodes the most part of the RBD and the partial downstream after RBD of the SARS-CoV-2 Delta S protein, but it started from the position downstream the start points "ATG" encoding for "M" of the S protein. So, the 813 nt insert-RFP fusing gene was only possible to express mRNA, but not to produce any fusing protein (Figure 3).

Designed shRNA targeting the conserved downstream RBD of the SARS-CoV-2 Delta S protein

The whole RNA genomes and their S protein genes of the SARS-CoV-2 variants were cluster analyzed. The S protein genes could be identified in their RNA genomes. In the SARS-CoV-2 Delta variant genome, the S protein gene (3816 nt) was started from 21517 nt and ended at 25332 nt. The RBD (317-539aa, described as the sequence in sp|P0DTC2|SPIKE_SARS2) from the coding region of the S protein (1271aa) of the genome (OL903477.1) was started from 22465 nt and ended at 23133 nt (Figure 4). Although there were different kinds of mutation in RBDs of the SARS-CoV-2 S proteins, the 813 nt cDNA sequence encoding for the part of the RBD region and the highly conserved partial downstream RBD of the SARS-CoV-2 Delta S protein gene was selected as the potential shRNA targets. The shRNA was designed on the base of the 813 nt insert sequence from the Delta. Considering of the shRNA to target not only the Delta, but also the Omicrons and the others, we finally picked up the highly conserved region at the downstream but

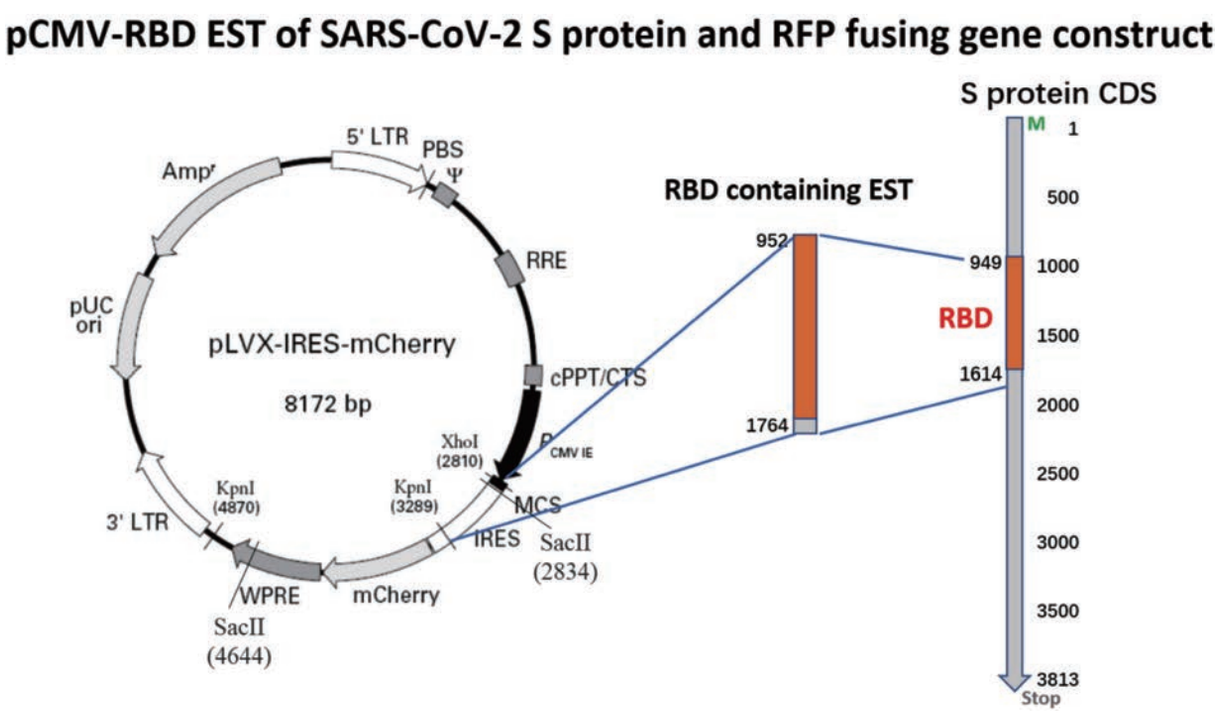

Fig. 2 Construction of pCMV-RBD EST of SARS-CoV-2 S protein and RFP fusing gene plasmid, named pCMV-S-protein-RBD-EST-RFP. The synthesized and annealed double strands of the DNA fragment was with a XhoI sticky site (CTCGAG) at the 5' end, KpnI sticky site (GGTACC) at the 3' end. The sense strand (813 nt) of the DNA fragment encodes for the most part of the RBD of the SARS-CoV-2 Delta S protein. The 3' LTR acts as a polyadenylation signal to terminate transcription.

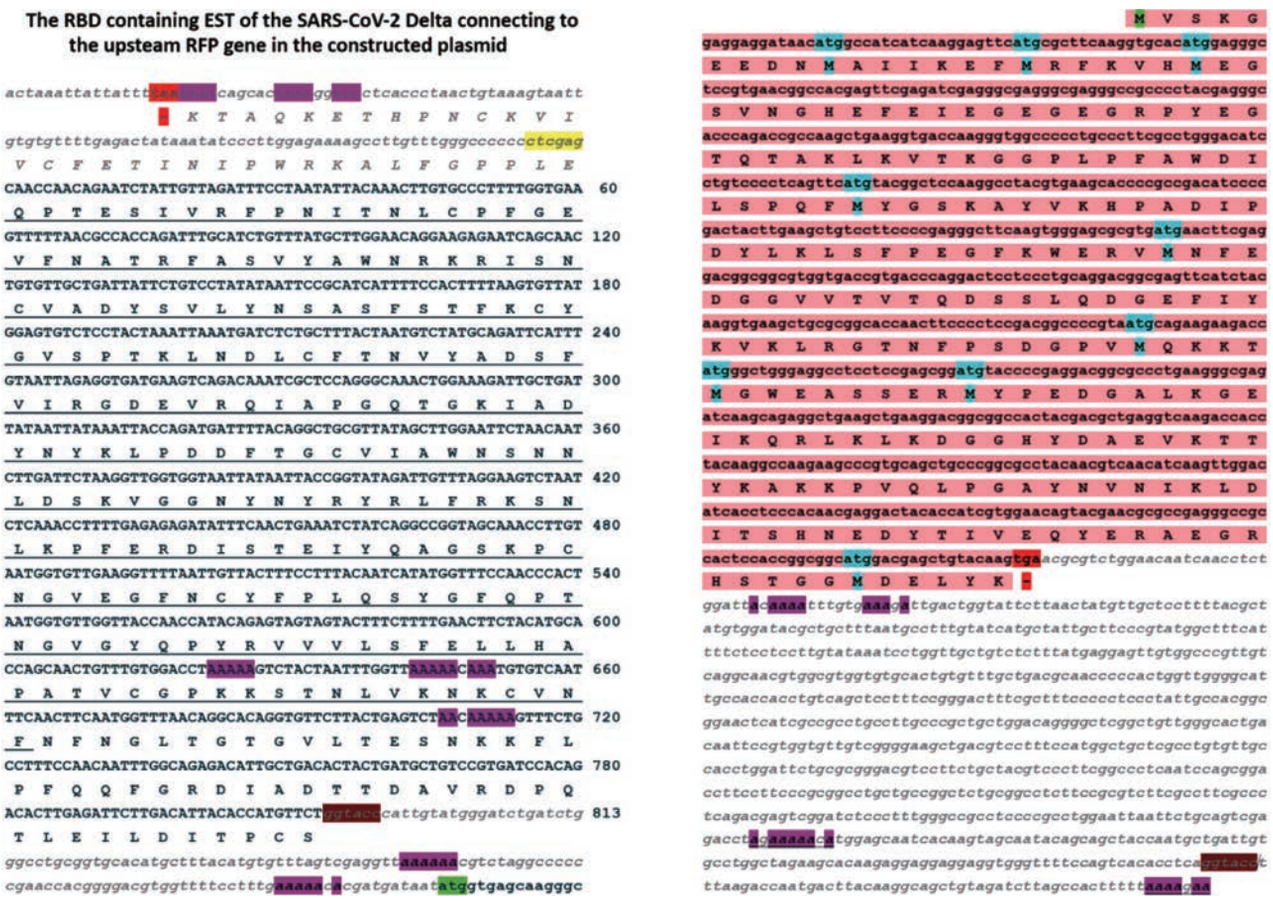

Fig. 3 The EST insert encoding for the RBD and the downstream RBD of the SARS-CoV-2 Delta S protein connected to upstream RFP gene was confirmed by Sanger sequencing. The insert is between the restriction sites of the XhoI (CTCGAG, with yellow background) at 5' end and KpnI (GGTACC, with brown background) at 3' end. The insert region theoretical encoding for the RBD (with underline) and the downstream (after the RBD region and before the KpnI restriction site (GGTACC, with brown background) of the S protein Delta. However, there is no "ATG" for this RBD and whole fusion gene in the part of the EST of the S protein Delta. The RFP protein was translated from its own "ATG" for its entire protein as wild-type RFP protein.

near the RBD of the S protein genes to test (Figure 4). The shRNA, named as shRNA688, was with the sense sequence as "GGTGT TCTTA CTGAG TCTAA C" which was total identity in all the downstream the RBDs of the S protein genes of SARS-CoV-2 variants (Figure 5).

The constructed EGFP marker gene and the shRNA688 targeting the S protein gene of the SARS-CoV-2 co-expressing plasmid

The constructed pCMV-EGFP-pH1-shRNA688 co-expression plasmid was prepared on the base of the pSIL-EGFP vector which contained pCMV-EGFP gene for gene transfection marker gene. The H1 promoter (108 bp), one of the human RNA polymerase III type promoters, was used in the upstream shRNA688. The shRNA688 was in downstream the H1 promoter. There are 4 elements in shRNA688 cDNA. The sequences were as the sense "GGT GTT CTT ACT GAG TCT AAC", the loop "TTC AAG AGC", the antisense "GTT AGA CTC AGT AAG AAC ACC", and the termination "TTT TTT". Both H1 promoter and shRNA688 were confirmed by Sanger sequencing. The constructed plasmid was with the pCMV promoter to drive the EGFP marker gene expression and the human H1 promoter to drive the expression of the shRNA688 which were designed for targeting the S protein transcripts of the SARS-CoV-2 (Figure 6).

The HEK293T cells expressed both EGFP and RFP genes with the green and red fluorescence after co-transfection with pCMV-EGFP-pH1-shRNA and pCMV-S-protein-RBD-EST-RFP plasmids

The HEK293T cells were co-transfected with the pCMV-S protein RBD EST-RFP fusing gene plasmid and the pCMV-EGFP-pH1-shRNA688 plasmid

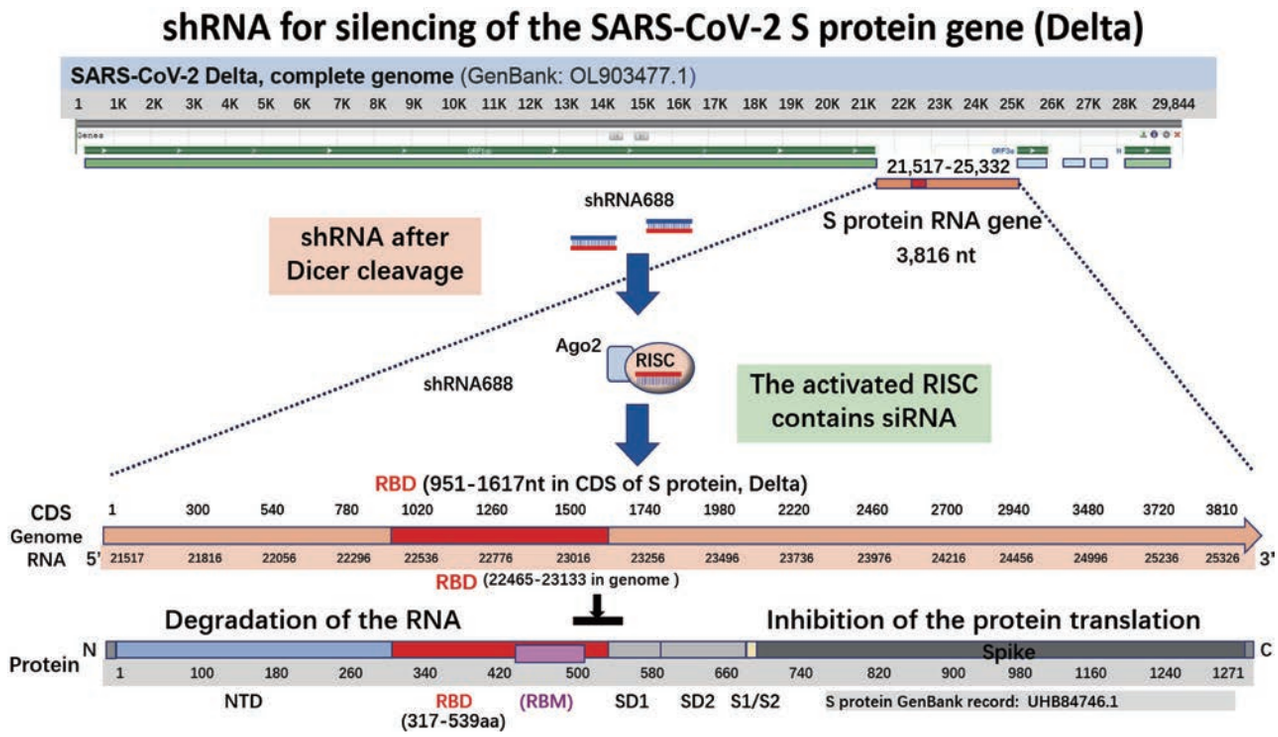

Fig. 4 shRNA targeting the S protein gene of the SARS-CoV-2 Delta. The location of the S protein gene and its encoded protein of SARS-CoV-2 Delta were indicated. The selected shRNA (shRNA688) was targeted the downstream but closed to the coding region of the RBD of the S protein of the SARS-CoV-2 Delta variant.

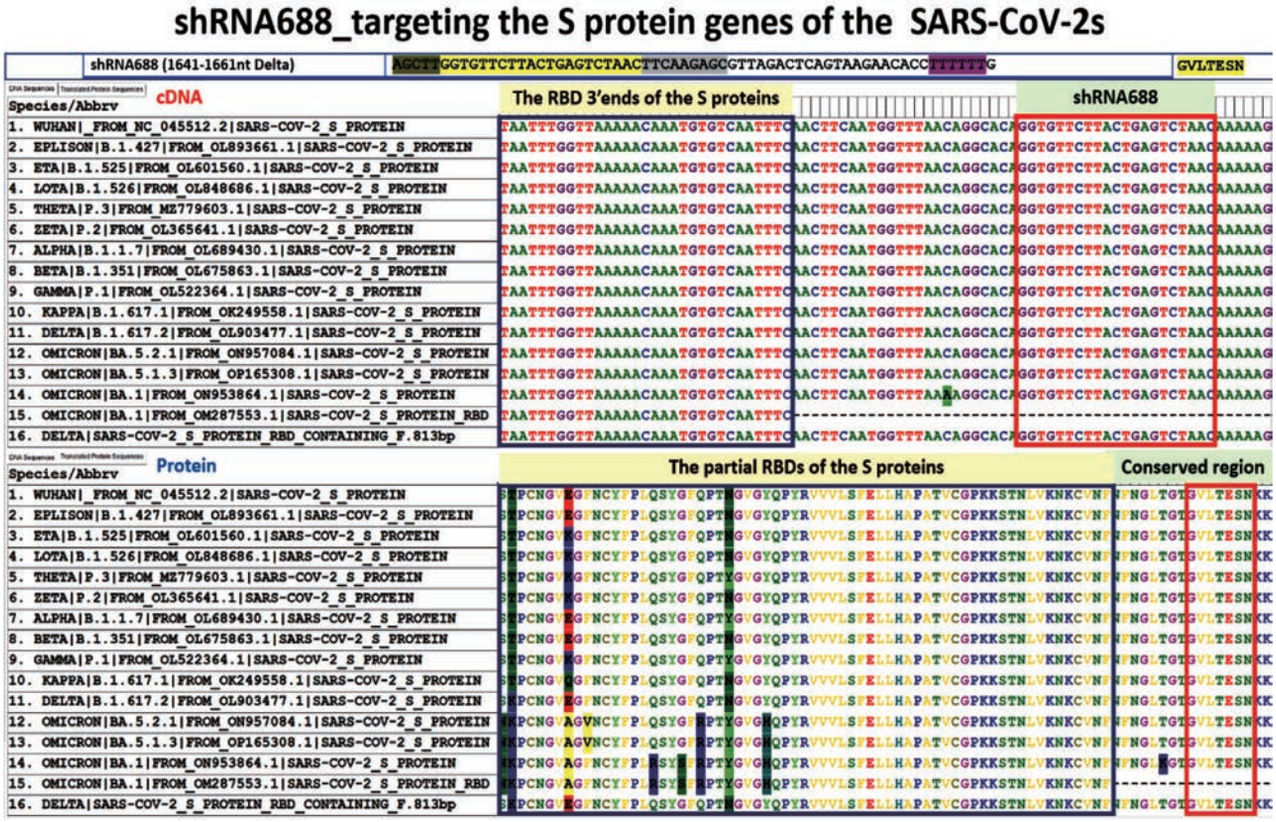

Fig. 5 shRNA688 targeting the downstream RBDs of S protein genes of the SARS-CoV-2s. The sense sequence of the shRNA688 was "GGT GTT CTT ACT GAG TCT AAC" which was total identity in all the downstream the RBDs of the S protein genes of SARS-CoV-2 variants (inside of the red line box, in up block). If the sense sequence of the shRNA688 was translated into peptide sequence as a reference, it was "GVLTESN" which was the same as the all the compared peptide sequences of the S protein isoforms although there were the mutations in the RBD peptide sequences of the S proteins of the SARS-CoV-2 variants.

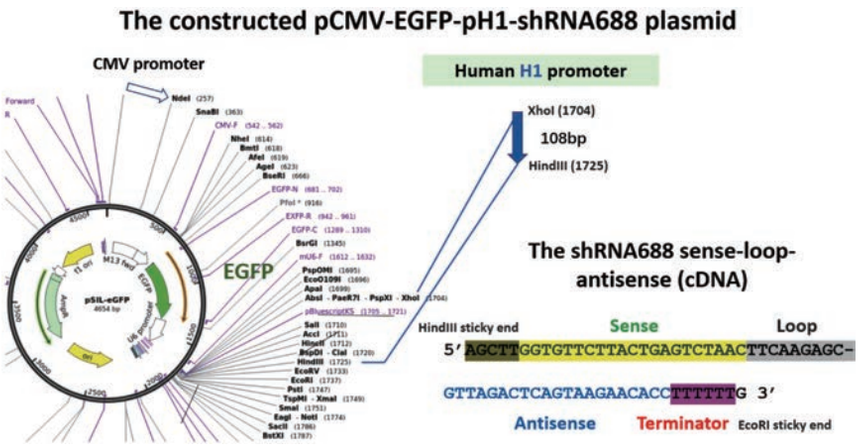

Fig. 6 The constructed EGFP marker gene and the shRNA688 targeting the S protein gene of the SARS-CoV-2 co-expressing plasmid, named as pCMV-EGFP-pH1-shRNA688. The pSIL-EGFP expression plasmid was used as a basic vector. The human H1 promoter (108 bp) was inserted into XhoI and HindIII restriction sites. The annealed double strands of the shRNA688 forward strand (with 4 elements indicated) and its reverse complementary strand with HindIII and EcoRI restriction sticky ends was integrated in downstream H1 promoter and confirmed by Sanger sequencing.

mediated with Lipofactamine 2000 as the ratio of the DNA to Liposome (1:3). After the transfection, there were three kinds of transfected cells. One kind of the transfected cells received the pCMV-S protein RBD EST-RFP fusing gene plasmid were with red fluorescence. The second kind of the transfected cells received the pCMV-EGFP-pH1-shRNA688 plasmid were with green florescence under fluorescence microscope. The third kind of the transfected cells were received both kinds of the plasmids. Such transfected cells expressed both red and green fluorescence as shown as yellow fluorescence after the fluorescent images were overlapped (Figure 7).

shRNA688 degraded the S protein Est in the gene transfected HEK293T determined by RT-qPCR

After the HEK293T cells were co-transfected with pCMV-EGFP-pH1-shRNA688 plasmid, and pCMV- S protein RBD containing EST-RFP fusing gene plasmid, the cells with both the green and red

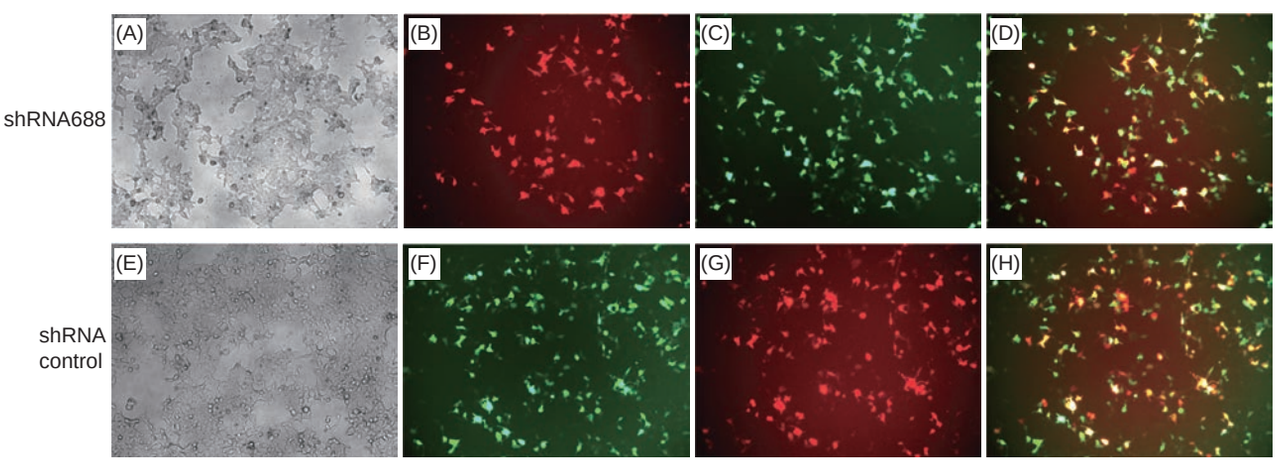

Fig. 7 The HEK293T cells were co-transfected with the pCMV-S protein RBD EST-RFP fusing gene plasmid and the pCMV-EGFP-pH1-shRNA688 plasmid. In shRNA testing, the cultured cells were transfected with the pCMV-EGFP-pH1-shRNA688 plasmid DNA. In the control, the cells were transfected with the pSIL-EGFP plasmid DNA, which was the empty backbone to construct shRNA silencing plasmids with EGFP transfection maker (https://www.addgene.org/52675/), respectively. The transfected cells were observed under fluorescence microscope with the filters for red or green fluorescence (10X objective, Leica). (A) HEK293T cells grew after co-transfection (under daylight). (B) The cells expressed the S protein RBD EST-RFP fusing gene with red fluorescence. (C) The cells expressed EGFP with green fluorescence. (D) When the cells in the culture were co-transfected with two kinds of the plasmids, some cells were with both red and green fluorescence as finally shown as yellow colors after the images B and C have been merged. (E) The cells grew after co-transfection. (F) Some cells were with red fluorescence. (G) Some cells were with green fluorescence. (H) Some cells were with yellow colors after the images F and G have been merged.

pH1-shRNA688 reduced of the amount of the S protein mRNA Est813 of the SARS-CoV-2

Exp.	Samples	S protein Mean Cp	S protein Cp SD	GAPDH Mean Cp	GAPSH Cp SD	ΔCT (S.P.-GAPDH)	Concentration (Target/Ref.)	Degradation rates
A	shRNA688 +S protein Est813	18.57	0.14	13.30	0.49	5.27	0.026	0.465
	Control +S protein Est813	17.34	0.37	13.17	0.39	4.17	0.056	
B	H1-shRNA688 +S protein Est813	18.84	0.52	14.11	1.00	4.73	0.038	0.531
	Control +S protein Est813	19.21	0.30	15.40	0.14	3.82	0.071	
C	H1-shRNA688 +S protein Est 813	15.24	0.44	12.10	0.37	3.14	0.114	0.462
	Control +S protein Est813	14.03	0.26	12.00	0.21	2.02	0.246	

0.486 ± 0.039

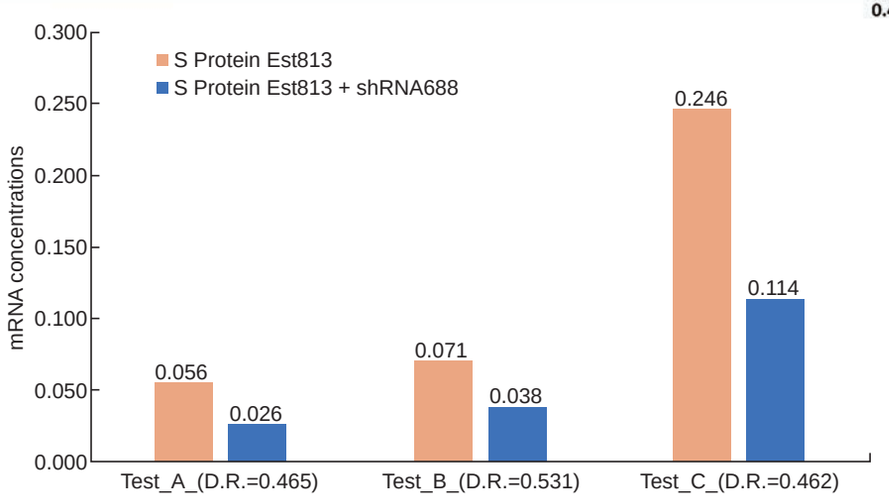

Fig. 8 The mRNA concentration of the S protein mRNA Est813 in transfected cells after shRNA688 treatment was significantly reduced compared to the control. Results showed that the three times of RT-qPCR experiments. The degradation rates of the mRNA concentration of the S protein mRNA Est813 after shRNA688 treatment were shown down till in A: 0.465, B: 0.531 and C: 0.462 (data were triplicated) compared to the control. The average and standard error degradation rate of the three-time experiments were down to 0.4860.039. As the concentration of the S protein mRNA Est813 in each experiment were varied but the degradation rates (D.R) were in similar levels. The data were also shown in graphics.

fluorescence. The total RNA from each transfection were isolated and cDNA were prepared. The RT-qPCR were performed, and the data were statistically analyzed. The experiments were performed repeatedly three times and each experiment was with samples (n = 3). The results showed that the average and standard error of the degradation rate of the transcripts of the S protein Est (813 bp) after shRNA688 treatment was down to 0.4860.039 compared to the control. The results indicated that the transcript concentration of the S protein mRNA Est (813 bp) in transfected cells after shRNA688 treatment was significantly reduced comparing to the control (Figure 8).

Conclusions

The constructed shRNA688 was targeting the highly conserved region of the S protein genes of the SARS-CoV-2

The SARS-CoV-2 with novel mutations have resulted in the COVID-19 pandemic world-wide so far (1). In this study, we took an 813 nt fragment of the S protein gene from the SARS-CoV-2 Delta as shRNA target. The 813 nt contained the most part of RBD and partial downstream RBD of S protein gene. Based on this 813 nt fragment sequence, we have designed, prepared the shRNA688 and performed the RNAi experiments. Our results showed that the shRNA688 significantly reduced the concentration of the S protein mRNA Est813 transcripts. We analyzed the different types of S protein CDS and protein isoforms. The results showed that shRNA688 targeting region was highly conserved in all SARS-CoV-2 variants, including the Delta, Omicron BA.1, Omicron BA.5.1.3 and Omicron BA.5.2.1 which were caused the COVID-19 in recent two years. So, the shRNA688 not only degraded S protein mRNA Est of the SARS-CoV-2 Delta in our study, but also theoretically has the RNAi function on all existed SARS-CoV-2 variants identified so far, as the target region of shRNA688

were shared in all S protein genes of the SARS-CoV-2 variants.

Co-transfection of the shRNA and EGFP expression plasmid, and S protein gene fragment-RFP fusing gene plasmid in human cell line as a useful cell experimental model for RNAi research

Considering the lab biosafety, we constructed the pCMV-S protein RBD containing EST-RFP fusing gene plasmid and sent the fragment of S protein gene into experimental cells. We were carefully to pick the fragment and connected with the RFP gene as a fusing gene, which did not produce any fusing protein, but produce the wild-type RFP gene as gene transfection marker. If the transfected cells expressed the constructed S protein RBD containing EST-RFP fusing gene, the cells were with red florescence. Considering the delivery efficiency of shRNA for RNAi, we constructed the pCMV-EGFP-pH1-shRNA plasmid. In one construct, pCMV derived EGFP expression, the human H1 promoter drives the shRNA expression. We used LipofectAMINE2000 to mediate both pCMV-S protein RBD containing EST-RFP fusing gene plasmid and pCMV-EGFP-pH1-shRNA plasmid into the cultured cells. The gene transfection ratios can be easily observed under fluorescence microscope. The co-transfection efficiency can be observed by image merging analysis of the red fluorescence and the green fluorescence. The co-transfected cells with yellow color about average 20-30% were under the consideration of performing RT-qPCR to determine the mRNA concentration of the targeted S protein Est fusion gene transcripts, to test the RNAi effects of the shRNA. Here, the shRNA688 reported by us in this study, as we have observed the RNAi results of shRNA688, we did not try to sort both the red or the green florescence gene expressed cells by Flow cytometry (FASC).

shRNA688 could be potential therapeutic drugs against SARS-CoV-2

The SARS-CoV-2 is RNA genome virus. When the SARS-CoV-2 have infected human lung epithelial cells, the virus genetic RNA invaded the infected cells. The S protein of the virus was translated from the S protein RNA gene. In this study, we used the shRNA688 to degrade the transcripts of the S protein RBD containing EST-RFP fusing gene in cell model successfully, although we did not perform any experiment on real SARS-CoV-2 to investigate whether the full RNA genome of the SARS-CoV-2 can be degraded or not by shRNA688. As we all know, several variants of the SARS-CoV-2 were already existed. Since the spread of SARS-CoV-2, the vaccines and neutralizing antibodies were research hot fields. It takes us great efforts and time to prepare and update the vaccines or identify novel neutralizing antibodies to avoid the immune escapes of the developed neutralizing antibodies to the new mutant antigens of the S proteins of the SARS-CoV-2 novel variants. Nowadays, a novel variant of the SARS-CoV-2 can be fully sequenced and analyzed. If any virus mutants exist in the targeted RNA sequence, the RNAi element can be also easily and quickly designed and prepared to test its RNAi function on the potential new mutants of SARS-CoV-2. At present, the Food and Drug Administration (FDA) has issued emergency approval for the use of some antiviral drugs. RNAi based therapy provides a tractable target for antiviral treatment. The use of nanoparticles as carriers for the delivery of siRNAs to specific cells of the human body could play a crucial role in the specific therapy of SARS-CoV-2 infections (35). For real clinical application, the optimal nanomaterials or mediators will be under consideration for aerosol inhaler. Inhaled siRNA holds great promise to develop antiviral therapies for respiratory diseases. COVID-19 caused by the SARS-CoV-2 virus is a fast-emerging disease with even deadly consequences. The pulmonary system and lungs are most prone to damage caused by certain the SARS-CoV-2 infection, which leaves a destructive footprint in the lung tissue, making it incapable of conducting its respiratory functions and resulting in severe acute respiratory disease and loss of life. The RNAi can be employed to develop therapies against the virus. This approach allows specific binding and silencing of therapeutic targets by using shRNA molecules. the feasibility of delivering promising therapies by the inhalational route, with the expectation that this route will provide one of the effective interventions to halt viral spread (36). The short double strands of shRNA will be under consideration to instead of the plasmids. Furthermore, to collaboratively test RNAi drug function on the pseudovirus, or even the SARS-CoV-2 are supposed with the research groups in the biosafety labs. Once a pipeline of siRNA design and delivery to the respiratory tract is established, the adaptation of RNAi-based therapies to new targets is comparably simple. Thus, it could allow a relatively fast development of

antiviral drugs in emergency settings caused by newly emerging pathogens affecting the respiratory tract such as SARS-CoV-2 (37). We hope that RNAi can be developed as one of the effective drugs for treating SARS-CoV-2 to save the lives of patients.

Acknowledgments

This research was supported by the Ministry of Science and Technology of China, Nantong Science and Technology Bureau (NT-HM-2020-09-24), the Shanghai Jingong Construction (Group) Health Fund (SHJG-2021-0402), and the Yangtze River Delta Drug Advanced Research Institute Foundation (NT-CGY202103).

Conflict of Interests

Genome-decoding (Jiangsu Zhongfang Gene) Biomedical Technology company have a patent application for shRNA688-against SARS-CoV-2.

References

[1] Zhu, N., Zhang, D., Wang, W., Li, X., Yang, B., Song, J., Zhao, X., Huang, B., Shi, W., Lu, R. *et al.* A Novel Coronavirus from Patients with Pneumonia in China, 2019. *N Engl J Med*, 2020, 382: 727-733.

[2] Zhu, C., Lee, J.Y., Woo, J.Z., Xu, L., Nguyenla, X., Yamashiro, L.H., Ji, F., Biering, S.B., Van Dis, E., Gonzalez, F. *et al.* An intranasal ASO therapeutic targeting SARS-CoV-2. *Nat Commun*, 2022, 13: 4503.

[3] Chang, Y.C., Yang, C.F., Chen, Y.F., Yang, C.C., Chou, Y.L., Chou, H.W., Chang, T.Y., Chao, T.L., Hsu, S.C., Ieong, S.M. *et al.* A siRNA targets and inhibits a broad range of SARS-CoV-2 infections including Delta variant. *EMBO Mol Med*, 2022, 14: e15298.

[4] Wouters, O.J., Shadlen, K.C., Salcher-Konrad, M., Pollard, A.J., Larson, H.J., Teerawattananon, Y. and Jit, M. Challenges in ensuring global access to COVID-19 vaccines: production, affordability, allocation, and deployment. *The Lancet*, 2021, 397: 1023-1034.

[5] Kuzmina, A., Khalaila, Y., Voloshin, O., Keren-Naus, A., Boehm-Cohen, L., Raviv, Y., Shemer-Avni, Y., Rosenberg, E. and Taube, R. SARS-CoV-2 spike variants exhibit differential infectivity and neutralization resistance to convalescent or post-vaccination sera. *Cell Host Microbe*, 2021, 29: 522-528, e522.

[6] Cao, Y., Wang, J., Jian, F., Xiao, T., Song, W., Yisimayi, A., Huang, W., Li, Q., Wang, P., An, R. *et al.* Omicron escapes the majority of existing SARS-CoV-2 neutralizing antibodies. *Nature*, 2022, 602: 657-663.

[7] McMillan, N.A.J., Morris, K.V. and Idris, A. (2022) RNAi to treat SARS-CoV-2-variant proofing the next generation of therapies. *EMBO Mol Med*, 2022, 14: e15811.

[8] Traube, F.R., Stern, M., Tolke, A.J., Rudelius, M., Mejias-Perez, E., Raddaoui, N., Kummerer, B.M., Douat, C., Streshnev, F., Albanese, M. *et al.* Suppression of SARS-CoV-2 Replication with Stabilized and Click-Chemistry Modified siRNAs. *Angew Chem Int Ed Engl*, 2022: e202204556.

[9] Merkel, O.M. Can pulmonary RNA delivery improve our pandemic preparedness? *J Control Release*, 2022, 345: 549-556.

[10] Lin, P., Shen, G., Guo, K., Qin, S., Pu, Q., Wang, Z., Gao, P., Xia, Z., Khan, N., Jiang, J. *et al.* Type III CRISPR-based RNA editing for programmable control of SARS-CoV-2 and human coronaviruses. *Nucleic Acids Res*, 2022, 50: e47.

[11] Setten, R.L., Rossi, J.J. and Han, S.P. The current state and future directions of RNAi-based therapeutics. *Nat Rev Drug Discov*, 2019, 18: 421-446.

[12] Hu, B., Zhong, L., Weng, Y., Peng, L., Huang, Y., Zhao, Y. and Liang, X.J. Therapeutic siRNA: state of the art. *Signal Transduct Target Ther*, 2020, 5: 101.

[13] Carthew, R.W. and Sontheimer, E.J. Origins and Mechanisms of miRNAs and siRNAs. *Cell*, 2009, 136: 642-655.

[14] Berber, B., Aydin, C., Kocabas, F., Guney-Esken, G., Yilancioglu, K., Karadag-Alpaslan, M., Caliseki, M., Yuce, M., Demir, S. and Tastan, C. Gene editing and RNAi approaches for COVID-19 diagnostics and therapeutics. *Gene Ther*, 2021, 28: 290-305.

[15] Chowdhury, U.F., Sharif Shohan, M.U., Hoque, K.I., Beg, M.A., Sharif Siam, M.K. and Moni, M.A. A computational approach to design potential siRNA molecules as a prospective tool for silencing nucleocapsid phosphoprotein and surface glycoprotein gene of SARS-CoV-2. *Genomics*, 2021, 113: 331-343.

[16] Donia, A. and Bokhari, H. RNA interference as a promising treatment against SARS-CoV-2. *Int Microbiol*, 2021, 24: 123-124.

[17] Fu, Y. and Xiong, S. Tagged extracellular vesicles with the RBD of the viral spike protein for delivery of antiviral agents against SARS-COV-2 infection. *J Control Release*, 2021, 335: 584-595.

[18] Abdullah Al Saba, M., Sajib Chakraborty, AHM Nurun Nabi Prediction of putative potential siRNAs for inhibiting SARS-CoV-2 strains, including variants of concern and interest. *Future Microbiol*, 2022, 17: 15.

[19] Sohrab, S.S., El-Kafrawy, S.A. and Azhar, E.I. Effect of insilico predicted and designed potential siRNAs on inhibition of SARS-CoV-2 in HEK-293 cells. *J King Saud Univ Sci*, 2022, 34: 101965.

[20] Khaitov, M., Nikonova, A., Shilovskiy, I., Kozhikhova, K., Kofiadi, I., Vishnyakova, L., Nikolskii, A., Gattinger, P., Kovchina, V., Barvinskaia, E. *et al.* Silencing of SARS-CoV-2 with modified siRNA-peptide dendrimer formulation. *Allergy*, 2021, 76: 2840-2854.

[21] Baldassi, D., Ambike, S., Feuerherd, M., Cheng, C.C., Peeler, D.J., Feldmann, D.P., Porras-Gonzalez, D.L., Wei, X., Keller, L.A., Kneidinger, N. *et al.* Inhibition of SARS-CoV-2 replication in the lung with siRNA/VIPER polyplexes. *J Control Release*, 2022, 345: 661-674.

[22] Friedrich, M., Pfeifer, G., Binder, S., Aigner, A., Vollmer Barbosa, P., Makert, G.R., Fertey, J., Ulbert, S., Bodem, J., Konig, E.M. *et al.* Selection and Validation of siRNAs Preventing Uptake and Replication of SARS-CoV-2. *Front Bioeng Biotechnol*, 2022, 10: 801870.

[23] Becker, J., Stanifer, M.L., Leist, S.R., Stolp, B., Maiakovska, O., West, A., Wiedtke, E., Borner, K., Ghanem, A., Ambiel, I. *et al.* Ex vivo and in vivo suppression of SARS-CoV-2 with combinatorial AAV/RNAi expression vectors. *Mol Ther*, 2022, 30: 2005-2023.

[24] Ambike, S., Cheng, C.C., Feuerherd, M., Velkov, S., Baldassi, D., Afridi, S.Q., Porras-Gonzalez, D., Wei, X., Hagen, P., Kneidinger, N. *et al.* Targeting genomic SARS-

CoV-2 RNA with siRNAs allows efficient inhibition of viral replication and spread. *Nucleic Acids Res*, 2022, 50: 333-349.

[25] Roden, C.A., Dai, Y., Giannetti, C.A., Seim, I., Lee, M., Sealfon, R., McLaughlin, G.A., Boerneke, M.A., Iserman, C., Wey, S.A. *et al.* Double-stranded RNA drives SARS-CoV-2 nucleocapsid protein to undergo phase separation at specific temperatures. *Nucleic Acids Res*, 2022, 50:8168-8192.

[26] Dutta, N.K., Mazumdar, K. and Gordy, J.T. The Nucleocapsid Protein of SARS-CoV-2: a Target for Vaccine Development. *J Virol*, 2020: 94.

[27] Manfredonia, I., Nithin, C., Ponce-Salvatierra, A., Ghosh, P., Wirecki, T.K., Marinus, T., Ogando, N.S., Snijder, E.J., van Hemert, M.J., Bujnicki, J.M. *et al.* Genome-wide mapping of SARS-CoV-2 RNA structures identifies therapeutically-relevant elements. *Nucleic Acids Res*, 2020, 48: 12436-12452.

[28] Vandelli, A., Monti, M., Milanetti, E., Armaos, A., Rupert, J., Zacco, E., Bechara, E., Delli Ponti, R. and Tartaglia, G.G. Structural analysis of SARS-CoV-2 genome and predictions of the human interactome. *Nucleic Acids Res*, 2020, 48: 11270-11283.

[29] Hoffmann, M., Kleine-Weber, H., Schroeder, S., Kruger, N., Herrler, T., Erichsen, S., Schiergens, T.S., Herrler, G., Wu, N.H., Nitsche, A. *et al.* SARS-CoV-2 Cell Entry Depends on ACE2 and TMPRSS2 and Is Blocked by a Clinically Proven Protease Inhibitor. *Cell*, 2020, 181: 271-280 e278.

[30] Prandi, I.G., Mavian, C., Giombini, E., Gruber, C.E.M., Pietrucci, D., Borocci, S., Abid, N., Beccari, A.R., Talarico, C. and Chillemi, G. Structural Evolution of Delta (B.1.617.2) and Omicron (BA.1) Spike Glycoproteins. *Int J Mol Sci*, 2022: 23.

[31] Scovino, A.M., Dahab, E.C., Vieira, G.F., Freire-de-Lima, L., Freire-de-Lima, C.G. and Morrot, A. SARS-CoV-2's Variants of Concern: A Brief Characterization. *Front Immunol*, 2022, 13: 834098.

[32] Enjuanes, L., Sola, I., Zuniga, S., Honrubia, J.M., Bello-Perez, M., Sanz-Bravo, A., Gonzalez-Miranda, E., Hurtado-Tamayo, J., Requena-Platek, R., Wang, L. *et al.* Nature of viruses and pandemics: Coronaviruses. *Curr Res Immunol*, 2022, 3: 151-158.

[33] Vatandaslar, H. A Systematic Study on the Optimal Nucleotide Analogue Concentration and Rate Limiting Nucleotide of the SARS-CoV-2 RNA-Dependent RNA Polymerase. *Int J Mol Sci*, 2022, 23.

[34] Dai, F., Yusuf, F., Farjah, G.H. and Brand-Saberi, B. RNAi-induced targeted silencing of developmental control genes during chicken embryogenesis. *Dev Biol*, 2005, 285: 80-90.

[35] Zhang, Y., Almazi, J.G., Ong, H.X., Johansen, M.D., Ledger, S., Traini, D., Hansbro, P.M., Kelleher, A.D. and Ahlenstiel, C.L. Nanoparticle Delivery Platforms for RNAi Therapeutics Targeting COVID-19 Disease in the Respiratory Tract. *Int J Mol Sci*, 2022: 23.

[36] Uludağ, H., Parent, K., Aliabadi, H.M. and Haddadi, A. Prospects for RNAi Therapy of COVID-19. *Frontiers in Bioengineering and Biotechnology*, 2020: 8.

[37] Mehta, A., Michler, T. and Merkel, O.M. siRNA Therapeutics against Respiratory Viral Infections-What Have We Learned for Potential COVID-19 Therapies? *Adv Healthc Mater*, 2021, 10: e2001650.